

# The $\gamma p \rightarrow \pi^+ n$ Single Charged Pion Photoproduction.

W. Chen, H. Gao (co-spokesperson), X. Qian, Y. Qiang

Q. Ye, W. Z. Zheng, X. F. Zhu, X. Zong

*Triangle Universities Nuclear Lab, Duke University and*

*Department of Physics, Duke University, Durham, NC 27708*

M. Aghasyan, E. De Sanctis, M. Mirazita, S.A. Pereira, P. Rossi (co-spokesperson)

*INFN, Laboratori Nazionali di Frascati*

M. Battaglieri, R. De Vita

*INFN, sezione di Genova*

W. J. Briscoe, I. I. Strakovsky

*George Washington University*

T. Mibe

*KEK, Tsukubo, Ibaraki 205-0801, Japan*

S. Stepanyan

*Jefferson Lab*

A. Sibirtsev

*Forschungszentrum Jülich, Jülich, Germany*

D. Dutta (co-spokesperson)

*Mississippi State University*

A. Deppman, J. de Oliveira Echeimberg

*Universidade de São Paulo, São Paulo, Brasil*

and the **CLAS Collaboration**

PACS numbers:

## ABSTRACT

The  $\gamma n \rightarrow \pi^- p$  and  $\gamma p \rightarrow \pi^+ n$  reactions are essential probes of the transition from meson-nucleon degrees of freedom to quark-gluon degrees of freedom in exclusive processes. Following the Hall A experiment E94-104 on the study of the  $\gamma n \rightarrow \pi^- p$  process, preliminary CLAS g10 results confirm the E94-104 observation of a broad resonance structure around a center-of-mass energy of 2.2 GeV and a drastic drop of the differential cross-section in a narrow energy window of 300 MeV for a pion center-of-mass angle of  $90^\circ$ . Further, the preliminary CLAS g10 data show a new center-of-mass angle dependent resonance structure and the exact nature of it needs to be further investigated. We propose to carry out measurements in CLAS using a tagged photon beam on the  $\gamma p \rightarrow \pi^+ n$  process in fine photon energy and pion center-of-mass angular bins. Such measurements allow for the investigation of a possible angular dependent resonance structure in this channel and its isospin dependence, and the investigation of the onset of the scaling behavior. The proposed experiment requires a single charged particle trigger, 100 hours ( $\approx 4$  days) of CW electron beam at  $E_0 = 5.7$  GeV with 25 nA current on a 40 cm liquid hydrogen target.

## INTRODUCTION

The interplay between the nucleonic and partonic pictures of the strong interaction represents one of the major issues in contemporary nuclear physics. Although standard nuclear models are successful in describing the interactions between hadrons at large distances, and Quantum Chromodynamics (QCD) accounts well for the quark interactions at short distances, the physics connecting the two regimes remains unclear. In fact, the classical nucleonic description must break down once the probing distances become comparable to those separating the quarks. The challenge is to study this transition region by looking for the onset of some experimentally accessible phenomena naturally predicted by perturbative QCD (pQCD). The simplest is the constituent counting rule (CCR) for high energy exclusive reactions [1], in which  $d\sigma/dt \propto s^{-n+2}$ , with  $n$  the total number of point-like particles and gauge fields in the initial plus final states. Here  $s$  and  $t$  are the invariant Mandelstam variables for the total energy squared and the four-momentum transfer squared, respectively. Many exclusive reactions [2] at high energy and large momentum transfer appear to obey the CCR and in recent years, a similar trend, i.e. global scaling behavior, has been observed in deuteron photo-disintegration experiments [3] - [6] and in photo-production of charged pions [7] at a surprisingly low transverse momentum value of  $\sim 1.1$  (GeV/c)<sup>2</sup>.

The same dimensional analysis which predicts the quark counting rule also predicts hadron helicity conservation (HHC) for exclusive processes at high energy and large momentum transfers. However, polarization measurements on deuteron photo-disintegration [8], recently carried out in Hall A at Jefferson Lab (JLab), show disagreement with hadron helicity conservation in the same kinematic region where the quark counting behavior is apparently observed. These paradoxes make it essential to understand the exact mechanism governing the early onset of scaling behavior. Even though the global  $s$ -dependence of the cross-section for exclusive processes such as the pion-photoproduction display the expected scaling behavior, no definitive conclusion about the onset of partonic mechanisms can be made. This problem stems from the lack of theoretical calculations of the absolute cross-section and the lack of a complete set of experimental data to enable a detailed treatment of all resonant contributions. In addition to the onset of scaling, the recent data from JLab Hall-A experiment E94-104 also show dramatic changes in the scaled differential cross-section of charged pion photo-production in the center of mass energy range of 1.8 GeV to 2.4 GeV just before the onset of scaling. These data at 90° center-of-mass angle for both  $\pi^-$  and

$\pi^+$  photo-production seem to display a new resonant structure. This unexpected behavior has been confirmed by an analysis of the CLAS g10 data on the  $\gamma n \rightarrow \pi^- p$  process [9], which maps out both the energy and the angular dependence of the cross-section in very fine bins with high statistical precision. The g10  $\pi^-$  data also display a unique angular dependence in this center of mass energy range. The CLAS  $\pi^0$  photo-production data [10] confirm this resonance-like behavior. A definitive confirmation of this unique structure in the cross-section and a detailed extraction of the possible resonant contributions urgently awaits data on the  $\pi^+$  channel, which is lacking at present. This proposal aims to fill this gap with a high statistics measurement of the cross-section for the  $\gamma p \rightarrow \pi^+ n$  process, scanning with fine bins over both energy and center-of-mass angle.

Moreover, at higher energies in the scaling region a close examination of the agreement with the scaling expectations have shown oscillations about the scaling behavior. Historically, elastic proton-proton ( $pp$ ) scattering at high energies and large momentum transfer has played a very important role as they show substantial oscillations about the power law behavior. Oscillations are not restricted to the  $pp$  sector; they are also seen in  $\pi - p$  fixed angle scattering [11]. Exclusive  $\gamma N \rightarrow \pi N$  processes with their relatively slower fall-off with energy compared to other photon-induced processes are naturally advantageous to study possible oscillatory behavior around the quark counting rule prediction. Therefore along with the fine scan in the 1.8 - 2.4 GeV center of mass energy range, it is essential to extend the  $\gamma p \rightarrow \pi^+ n$  measurements to the highest energies available.

We propose to perform differential cross-section measurements of the  $\gamma p \rightarrow \pi^+ n$  process from hydrogen in Hall B using the CLAS detector, for photon energies between 1.14 to 5.4 GeV. In particular, we plan to map out the region of  $\sqrt{s} = 1.77 - 3.32$  GeV in fine energy bins and carry out an angular distribution study in a center-of-mass angular bin of  $5^\circ$  from  $50^\circ$  to  $115^\circ$ . These measurements will achieve the following goals:

- Detailed study of the resonance structure observed at higher center-of-mass energies and its angular dependent location shown by the  $\gamma n \rightarrow \pi^- p$  channel to investigate whether one observes similar features in the  $\gamma p \rightarrow \pi^+ n$  channel. The isospin dependence of such a structure will help unravel the nature of the observed resonance structure.
- Detailed investigation of the scaling behavior and the study of the scaling onset and

its connection to the pion transverse momentum.

- To investigate the possible oscillatory scaling behavior around the CCR prediction.

The proposal body is organized as following. Section II contains the physics motivations for the measurement, in Section III the proposed measurement is described and results from a Monte Carlo simulations of the experiment are reported, Section IV contains details of the experiment, evaluation of the counting rates and the beam time request, and Section V is the summary.

## PHYSICS MOTIVATIONS

### Constituent Counting Rule and Oscillations

The constituent counting rule predicts the energy dependence of the differential cross section at fixed center-of-mass angle for an exclusive two-body reaction at high energy and large momentum transfer as follows:

$$d\sigma/dt = h(\theta_{cm})/s^{n-2} \quad (1)$$

where  $h(\theta_{cm})$  depends on details of the dynamics of the process.

The quark counting rule was originally obtained based on dimensional analysis under the assumptions that the only scales in the system are momenta and that composite hadrons can be replaced by point-like constituents. Implicit in these assumptions is the approximation that the class of diagrams which represent on-shell independent scattering of pairs of constituent quarks (Landshoff diagrams) [12], can be neglected. Also neglected were contributions from quark orbital angular momentum which are power suppressed but can give rise to hadron helicity flipping amplitudes. Later on, these counting rules were confirmed within the framework of perturbative QCD analysis up to a logarithmic factor of  $\alpha_s$  and are believed to be valid at high energy in the perturbative QCD region. Such analysis relies on the factorization of the exclusive process into a hard scattering amplitude and a soft quark amplitude inside the hadron. Finally, in the last few years an all-orders demonstration of the counting rules for hard exclusive processes has been shown to arise from AdS/CFT [13]

which treats the conformal gauge field theory as dual of the string theory in anti-de Sitter space.

Although the quark counting rule agrees with data from a variety of exclusive processes, the other natural consequence of pQCD, i.e. the hadron helicity conservation selection rule (HHC), tends not to agree with data in the experimentally tested region, one recent example is the recoil polarization measurement from deuteron photodisintegration [8]. HHC arises from the fact that vector interactions (photon or gluon coupling with quarks) conserve chirality, leading to conservation of the sum of the components of the hadronic spins along their respective momentum directions, and of predictions of spin observables. In deriving this rule, higher orbital angular momentum states of quarks or gluons in hadrons and the effect of the hadron mass at high energies are neglected.

The elastic proton-proton ( $pp$ ) scattering at high energy and large momentum transfer has played a very important role in the study of the scaling behavior. A detailed investigation of the differential cross section of this process shows oscillations about the scaling behavior  $s^{-10}$  predicted by the quark counting rule [14]. Further, the spin correlation experiment in  $pp$  scattering first carried out at Argonne by Crabb *et al.* [15] shows striking behavior: at the largest momentum transfers ( $p_T^2 = 5.09 \text{ (GeV/c)}^2$ ,  $\theta_{c.m.} = 90^\circ$ ) it is  $\sim 4$  times more likely for protons to scatter when their spins are both parallel and normal to the scattering plane than when they are anti-parallel. Later spin-correlation experiments [16] confirm the early observation by Crabb *et al.* and showed that the spin correlation  $A_{NN}$  (given by  $\frac{\sigma(\uparrow,\uparrow) - \sigma(\uparrow,\downarrow)}{\sigma(\uparrow,\uparrow) + \sigma(\uparrow,\downarrow)}$ ) varies with energy about the pQCD prediction. Theoretical interpretation of this oscillatory behavior of the scaled cross-section ( $s^{10} \frac{d\sigma}{dt}$ ) and the striking spin-correlation in  $pp$  scattering was attempted by many authors. Some explained these features as the result of the interference between hard pQCD short-distance and long-distance (Landshoff) amplitudes [17], [18], [19]; others as the opening of a  $c\bar{c}uud\bar{u}ud$  resonant states [20].

Very recently, a number of new developments have generated renewed interest in this topic. Zhao and Close [21] have argued that a breakdown in the locality of quark-hadron duality (dubbed as “restricted locality” of quark-hadron duality) results in oscillations around the scaling curves predicted by the counting rule. They explain that the smooth behavior of the scaling laws arise due destructive interference between various intermediate resonance states in exclusive processes at high energies, however at lower energies this cancellation due to destructive interference breaks down locally and gives rise to oscillations about the

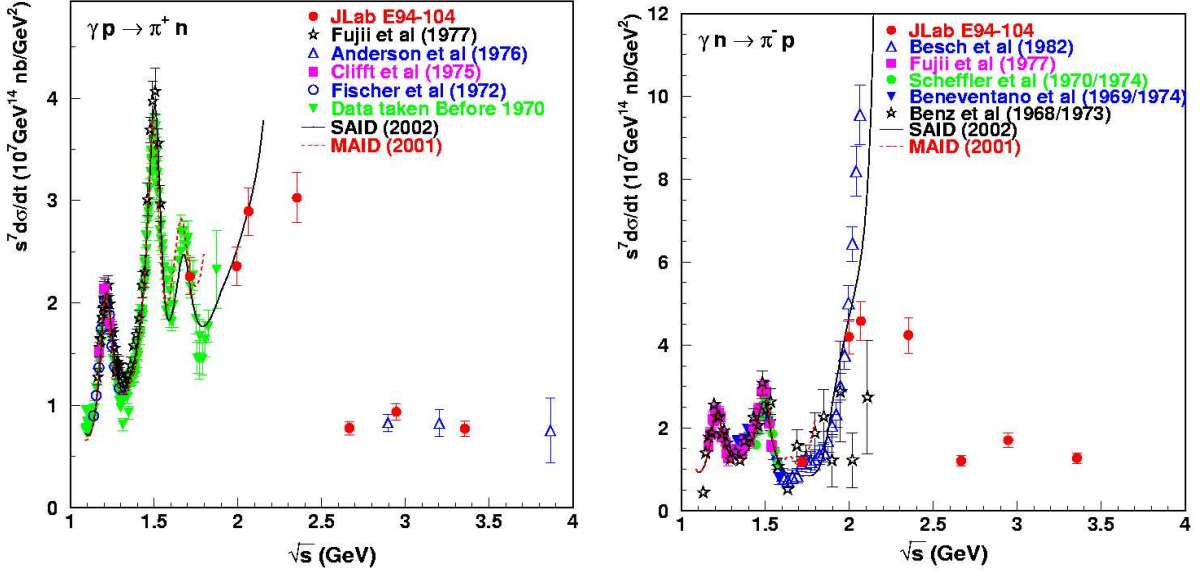


FIG. 1: The scaled differential cross section,  $s^7 \frac{d\sigma}{dt}$  as a function of  $\sqrt{s}$  at a center-of-mass angle of  $90^\circ$  for  $\gamma p \rightarrow \pi^+ n$  channel (left) and the  $\gamma n \rightarrow \pi^- p$  channel (right). The data from JLab E94-104 are shown as solid circles. The error bars for the new data and for the Anderson *et al.* data [24], include statistical and systematic uncertainties. Other data sets [11, 25] are shown with only statistical errors. The open squares (right panel) were averaged from data at  $\theta_{cm} = 85^\circ$  and  $95^\circ$  [26]. The solid line was obtained from the recent partial-wave analysis of single-pion photoproduction data [27] up to  $E_\gamma=2$  GeV, while the dashed line from the MAID analysis [28] up to  $E_\gamma=1.25$  GeV.

smooth behavior. On the other hand, Ji *et al.* [22] have derived a generalized counting rule based on pQCD analysis, by systematically enumerating the Fock components of a hadronic light-cone wave function. Their generalized counting rule for hard exclusive processes include parton orbital angular momentum and hadron helicity flip, thus they provide the scaling behavior of the helicity flipping amplitudes. The interference between the different helicity flip and non-flip amplitudes offers a new mechanism to explain the oscillations in the scaling cross-sections and spin correlations. Brodsky *et al.* [23] have used the anti-de Sitter/Conformal Field Theory correspondence or string/gauge duality [13] to compute the hadronic light front wave functions exactly and it yields an equivalent generalized counting rule without the use of perturbation theory.

Given that the nucleon photo-pion production has a much larger cross-section at high

energies ( $\frac{d\sigma}{dt} \propto \frac{1}{s^7}$ ), it is very desirable to use these reactions to investigate possible oscillatory scaling behavior. The precision data on  $\gamma p \rightarrow \pi^+ n$  and  $\gamma n \rightarrow \pi^- p$  were reported by JLab experiment E94-104 [7]. The results (Fig. 1) indicate the constituent counting rule behavior at center-of-mass angle of  $90^\circ$ , for photon energies above  $\sim 3$  GeV (i.e. above the resonance region). In addition to the  $s^{-7}$  scaling behavior, these data also suggest an oscillatory behavior. However, the rather coarse beam energy settings prevent a conclusive statement about the oscillatory behavior. Thus, to verify any structure in the scaled cross-section of photo-pion production processes, it is imperative that we do a fine scan of the scaling region for the  $\gamma p \rightarrow \pi^+ n$  and  $\gamma n \rightarrow \pi^- p$  processes. The relatively higher rates for these processes will also allow angular scans to investigate the momentum transfer ( $t$ ) and transverse momentum ( $p_T$ ) dependence of the scaling behavior in addition to the usual energy scan looking at the center-of-mass energy ( $W = \sqrt{s}$ ) dependence. Most importantly, such a measurement would allow us to study the new resonant structure observed in the  $\pi^-$  and  $\pi^0$  channels as described in the next section.

### Existing data on photopion production

Results from Experiment E94-104 carried out in Hall A at the JLab for single pion photo-production are shown in Figure 1. They agree with the world data within uncertainties in the overlapping region. The data at  $\theta_{cm} = 70^\circ, 90^\circ$  exhibit a global scaling behavior predicted by the constituent counting rule in both  $\pi^-$  and  $\pi^+$  channels. The data at  $\theta_{cm} = 50^\circ$  do not display scaling behavior and may require higher photon energies for the observation of the onset of the scaling behavior. The data suggest that a transverse momentum of around 1.2 GeV/c might be the scale governing the onset of scaling for the photo-pion production, which is consistent with what has been observed in deuteron photodisintegration [5, 6].

Beside the interest in looking for the onset of phenomena predicted by the pQCD, the study of the charged pions photo-production has also other appealing features. In fact, by looking at Fig. 1 the data below the scaling region show an interesting enhancement at a center-of-mass energy ranging approximately from 1.8 GeV to 2.5 GeV. This enhancement was seen in both channels of the charged pion photoproduction. One also notes a very striking feature from the data i.e. the scaled differential cross-section dropped by a factor of several units in a very narrow windows of the center of mass energy ( $\sim 200$ -300 MeV). With

the high statistics CLAS g10 data on the  $\gamma n \rightarrow \pi^- p$  process, these two interesting features have been firmly established.

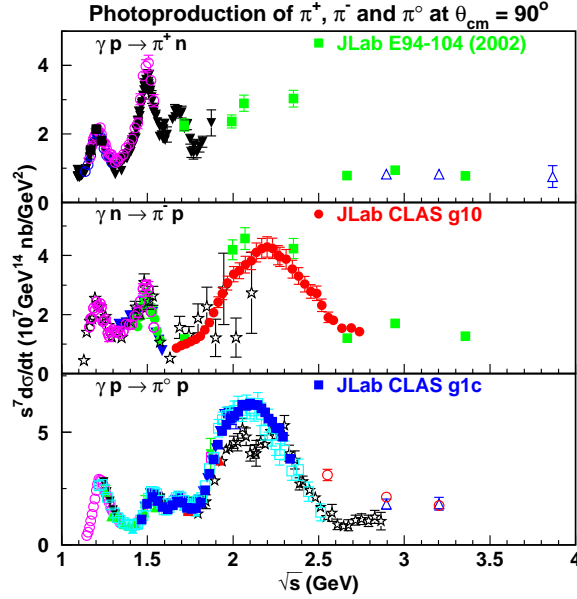


FIG. 2: Scaled differential cross-section  $s^7 \frac{d\sigma}{dt}$  as a function of center-of-mass energy  $\sqrt{s}$  for a pion center-of-mass angles of  $90^\circ$ . The upper panel is for the  $\gamma p \rightarrow \pi^+ n$  process, the middle panel is for the  $\gamma n \rightarrow \pi^- p$  process, and the lower panel is for the  $\gamma p \rightarrow \pi^0 p$  process. The green solid circles are results from [7], and the results from CLAS g10 [9] are shown as red solid circles. Results from Dugger *et al.* [10] on the neutral pion production are shown as blue solid squares. The blue open triangles are results from [24].

Fig. 2 shows the scaled differential cross-section  $s^7 \frac{d\sigma}{dt}$  as a function of center-of-mass energy  $\sqrt{s}$  for a pion center-of-mass angles of  $90^\circ$  for three different channels. The upper panel is for the  $\gamma p \rightarrow \pi^+ n$  process, the middle panel is for the  $\gamma n \rightarrow \pi^- p$  process, and the lower panel is for the  $\gamma p \rightarrow \pi^0 p$  process. The green solid circles are results from [7], the blue solid squares are results from Dugger *et al.* [10] on neutral pion production, and the results from CLAS g10 [9] are shown as red solid circles <sup>1</sup>. In both the  $\gamma p \rightarrow \pi^+ n$  and the  $\gamma p \rightarrow \pi^0 p$  channel, one sees clearly the  $\Delta$  resonance, the N(1500) and the N(1700) nucleon resonances. In the  $\gamma n \rightarrow \pi^- p$  channel, while one also sees the  $\Delta$  resonance and the N(1500)

<sup>1</sup> These results are currently being reviewed by the hadron spectroscopy working group of the CLAS Collaboration and therefore should be treated as preliminary.

resonance, one does not see the  $N(1700)$  resonance in the scaled differential cross-section. This is likely caused by the different isospin structure of the nucleon resonances around 1700 MeV. There are two distinct features shown in the data for all three channels: broad resonance structure around a center-of-mass energy of 2.1 GeV, and a drastic fall-off of the differential cross-section in a narrow energy window of about 300 MeV. The second feature was suggested by earlier Jefferson Lab experiment E94-104 [7] (shown as green solid circles), which now has been firmly established by results from CLAS g10 on the  $\gamma n \rightarrow \pi^- p$  as the data have very fine energy bins (Fig. 5), and also by the recent JLab CLAS results on the neutral pion production from proton [10]. Studies have been carried out to investigate whether such a resonance structure could be an artifact due to the scaling factor of  $s^7$  applied to the differential cross-section. The conclusion is the following. While a resonance peak position may shift slightly towards a higher mass due to the scaling, the  $s^7$  scaling factor alone could not produce a resonance structure, which is obvious because the  $s^7$  factor increases monotonically. Fig. 3 shows two cases for a single resonance structure and the effect on the mass peak shift due to the  $s^7$  scaling. The left panel is for a 2.0 GeV case and the right panel is for a 2.4 GeV resonance state. As shown the shift becomes smaller as the invariant mass of the resonance structure becomes larger and the shift is about 7 (17) MeV for a resonance state with a mass of 2.4 GeV and a width of 100 (150) MeV. Fig. 4 shows the effect of the  $s^7$  scaling on two Breit-Wigner resonances. In our study, we assumed two resonances with the higher mass resonance less pronounced in the spectrum. As one expects the scaling amplifies the higher mass resonance effect in the spectrum.

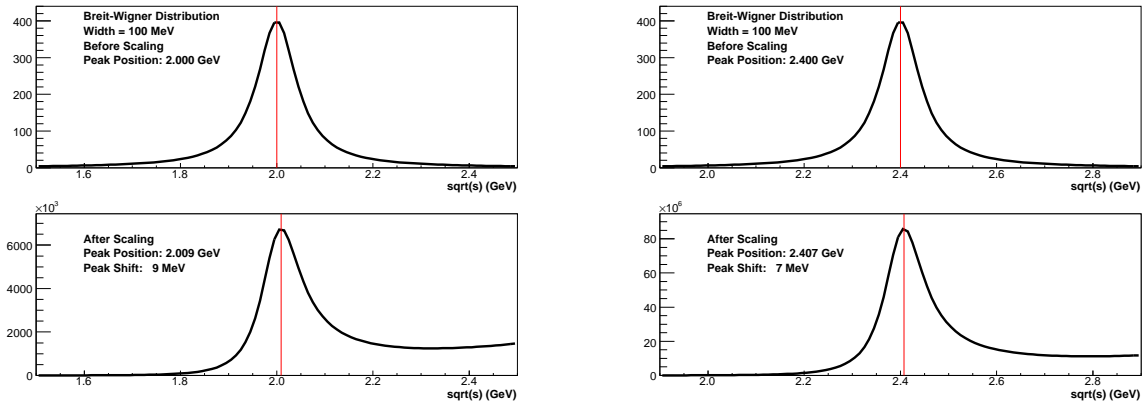


FIG. 3: Study of the  $s^7$  scaling effect on a Breit-Wigner resonance with a mass of 2.0 GeV (left) and 2.4 GeV (right).

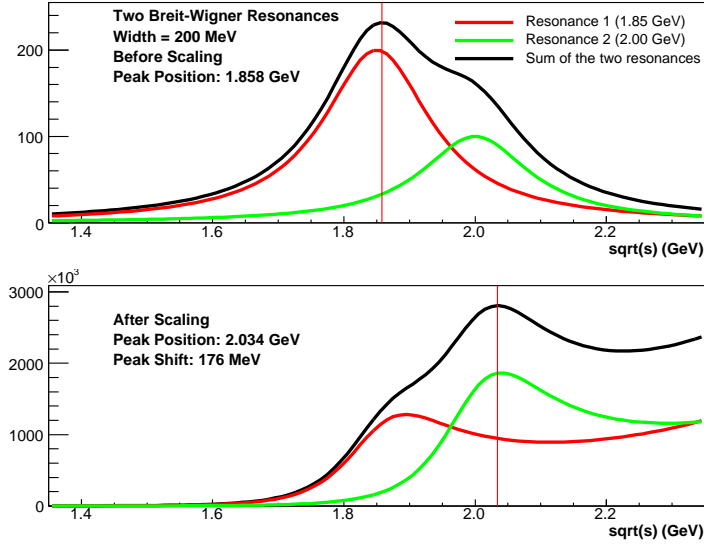


FIG. 4: Study of the  $s^7$  scaling effect on two Breit-Wigner resonances.

Without any conclusive statements at present, some speculations might be made. The observed enhancement around 2.2 GeV might relate to some unknown baryon resonances, as some of the well known baryon resonances ( $\Delta$ ,  $N^*$ 's around 1.2, 1.5 GeV and 1.7 GeV) are clearly seen in the scaled cross section below 2.2 GeV. Several baryon resonances are predicted to be in this energy region by the constituent quark model [29], but have not been seen (or firmly established) experimentally, i.e. the so called ‘missing resonances’. Recently, there has been evidence for the discovery of new resonances above 2 GeV from a number of experiments [25, 30, 31]. The BES Collaboration [30] reported evidence for a new resonance in the invariant mass spectrum of  $\pi^-p$  from the decay process of  $J/\Psi \rightarrow p\pi^-\bar{n}$ . This new resonance was determined to have a mass of  $2068 \pm 3_{-40}^{+15}$  MeV/ $c^2$ , and a width of  $165 \pm 14 \pm 40$  (MeV/ $c$ )<sup>2</sup> based on a simple Breit-Wigner fit. A partial wave analysis [30] concluded that this new  $N^*(2065)$  resonance can not be reproduced due to reflections from the established  $N^*$  resonances compiled by the Particle Data Group. The CB-ELSA Collaboration [31] reported from the  $p(\gamma, \eta)p$  process evidence of a new resonance  $N(2070)D_{15}$  with a mass and width of  $2068 \pm 22$ , and  $295 \pm 40$ , respectively. While the CB-Elsa collaboration [25] also reported evidence for the support of the new resonance  $N(2070)D_{15}$  from the  $\gamma p \rightarrow \pi^0 p$  process, the CLAS data on the same channel [10] does not show evidence for such a new resonance. The observed enhancement by E94-104 and CLAS g10 results [9] might also be associated with the strangeness production threshold [20, 32]. They could also be related to

the  $\phi$ -N bound state which has been predicted [33, 34].

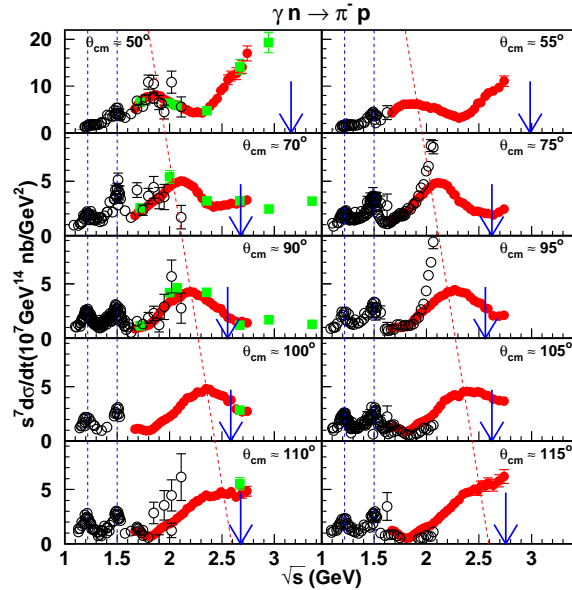


FIG. 5: The scaled differential cross-section  $s^7 \frac{d\sigma}{dt}$  for the  $\gamma n \rightarrow \pi^- p$  process as a function of center-of-mass energy  $\sqrt{s}$  for different pion center-of-mass angles: from  $50^\circ$  to  $115^\circ$ . The arrows indicate the location of  $\sqrt{s}$  corresponding to a transverse momentum value of 1.1 GeV/c. The green solid squares are results from [7]. The results from CLAS g10 [9] are shown as red solid circles.

Fig. 5 shows the scaled differential cross-section  $s^7 \frac{d\sigma}{dt}$  as a function of the center-of-mass energy  $\sqrt{s}$  for different pion center-of-mass angles: from  $50^\circ$  to  $115^\circ$  for the  $\gamma n \rightarrow \pi^- p$  process. The blue arrows indicate the location of  $\sqrt{s}$  corresponding to a transverse momentum value of 1.1 GeV/c. The transverse momentum has been shown as the physical quantity governing the onset of the scaling behavior, and 1.1 GeV/c is the onset value as demonstrated by experiments on deuteron photodisintegration [5, 6]. The green solid circles are results from [7]. The results from CLAS g10 are shown as red solid circles. The reach of the scaling region is clearly shown in the more backward angle kinematics: 70 to 110 degrees. In the forward angle of 50 degree, higher energies are necessary to reach a transverse momentum value of 1.1 GeV/c, required for the onset of the scaling behavior. A very unique angular-dependent feature is clearly shown in these data sets in the scaled differential cross-section. The aforementioned broad resonance structure around a  $\sqrt{s}$  value of 2.1 GeV at the pion center-of-mass angle of  $90^\circ$  seems to “be running” as a function of

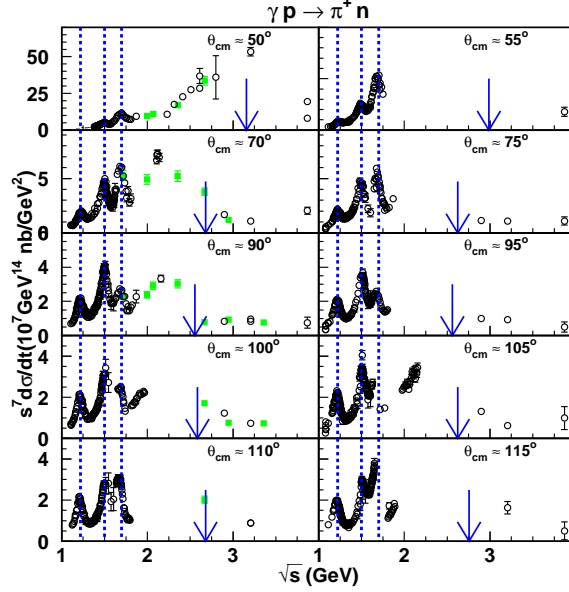


FIG. 6: The scaled differential cross-section  $s^7 \frac{d\sigma}{dt}$  for the  $\gamma p \rightarrow \pi^+ n$  as a function of center-of-mass energy  $\sqrt{s}$  for different pion center-of-mass angles: from  $50^\circ$  to  $115^\circ$ . The arrows indicate the location of  $\sqrt{s}$  corresponding to a transverse momentum value of 1.1 GeV/c. The green solid squares are results from [7]. The blue dotted lines indicate the locations of various nucleon resonance states.

the cms angle: from  $\sqrt{s}$  of 1.80 GeV at  $50^\circ$  to 2.45 GeV at  $105^\circ$  as shown by the red dotted lines. However, it is not clear whether this resonance behavior dies off for pion cms angle larger than  $105^\circ$  or it is “running” to further higher energies. The blue dotted lines indicate the locations of the  $\Delta$  and the  $N^*(1500)$  which do not change with respect to the pion cms angle as one expects. Fig. 6 is a similar plot for the  $\gamma p \rightarrow \pi^+ n$  process. Our studies have shown that such observed “running” behavior in the resonance like structure can not be produced due to the  $s^7$  scaling factor. Therefore, it is extremely important to carry out measurements on the  $\gamma p \rightarrow \pi^+ n$  process in fine energy bins as those of the g10 measurement and to much higher photon energies to determine the nature of this enhancement in the differential cross-section.

## Regge approach on charged pion photoproduction

Recently, a global analysis [35] of charged pion photoproduction based on Regge model has been carried out for photon energies between 3 to 8 GeV where nucleon resonance contributions are expected to be negligible. This allows for the extraction of the non-resonant background which can then be used to make prediction for photon energies below 3 GeV. The deviation between the data and the prediction can then be interpreted as possible signatures for excited baryon resonances. This is particularly the case of polarization observables and differential cross-section in the case of  $\pi^-$  photoproduction from the neutron thanks to the results from E94-104 [7] and CLAS g10 [9]. The situation for the  $\gamma p \rightarrow \pi^+ n$  channel is quite different. Therefore, it is essential to carry out the proposed experiment to remedy the situation with the lack of data for this process.

Figs 7, 8 show the differential cross-section  $\frac{d\sigma}{dt}$  for the  $\gamma p \rightarrow \pi^+ n$  process as a function of  $-t$  for different center-of-mass energies. Fig. 9, 10 show the corresponding plots for the  $\gamma n \rightarrow \pi^- p$  channel. While the Regge approach describes the data well at higher center-of-mass energies and lower  $-t$  region for both channels, the signature for baryon excitations is more pronounced in the  $\gamma n \rightarrow \pi^- p$  channel which is consistent with what we have seen in the CLAS g10 data and JLab Hall A data [7]. Therefore, it is extremely important to carry out the proposed measurements on the  $\gamma p \rightarrow \pi^+ n$  channel.

## THE PROPOSED MEASUREMENT

We propose to carry out a measurement of the photo-pion production cross-section for the fundamental  $\gamma p \rightarrow \pi^+ n$  process from a hydrogen target at a center-of-mass energy range  $\sim 1.77$  GeV to 3.32 GeV. This measurement is to be carried out in Hall B using the CLAS detector and the tagged photon beam. The large acceptance detection and a tagged photon capabilities have enormous advantages for doing the fine energy scan and the angular scan simultaneously. We plan to perform a detailed investigation of the scaled differential cross-section  $s^7 \frac{d\sigma}{dt}$  as a function of  $\sqrt{s}$  for the  $\gamma p \rightarrow \pi^+ n$  channel up to 3.32 GeV and a detailed study of the angular dependence of the scaling behavior will also be carried out. The data on the angular dependence can also be used to perform a partial wave analysis to determine the nature of the dramatic feature seen in the E94-104 data for the same process. Our

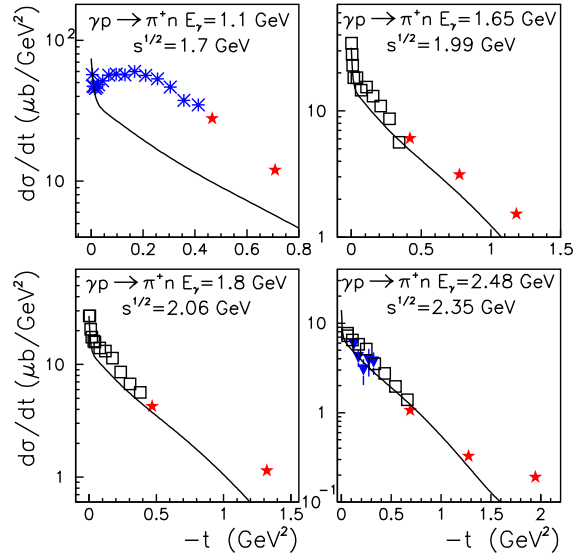


FIG. 7: The differential cross-section  $\frac{d\sigma}{dt}$  for the  $\gamma p \rightarrow \pi^+ n$  process as a function of  $-t$  for four different center-of-mass energies: 1.77, 1.99, 2.06, 2.35 GeV. The black solid curve is the Regge prediction discussed in the text and the red stars are data from Zhu *et al.* [7]. All other data are plotted as inverse triangles [36], asterisk [37] and open squares [38], respectively.

collaboration includes experts in partial wave analysis, for example the group from George Washington University.

For the process of interest,  $\gamma p \rightarrow \pi^+ n$ , one can use two-body kinematics to reconstruct the photon energy by detecting the  $\pi^+$  momentum and angle. The incident photon energy is known from the photon tagger. Thus, the redundancy in photon energy determination from the reconstructed photon energy based on the two-body process provides a crosscheck. This study will allow the detailed mapping of the dramatic transition region suggested by the Hall A E94-104 data [7]. It will also help confirm the oscillations in the scaled cross-section.

We have analyzed one run from the g11 running period where the trigger was set for single charged particles. This run had used a 25 nA electron beam on a 40 cm liquid hydrogen target. This gave a trigger rate of 4KHz. The sample spectra from this run are shown in Figure 11. The upper left panel shows the missing mass spectrum, where the recoiling neutron peak is clearly identifiable. The upper right panel shows a plot of photon energy versus missing mass and once again shows the neutron events (from the  $\gamma p \rightarrow \pi^+ n$  process)

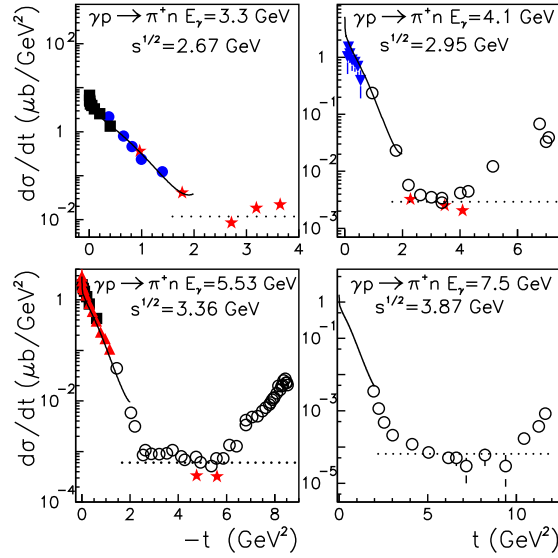


FIG. 8: The differential cross-section  $\frac{d\sigma}{dt}$  for the  $\gamma p \rightarrow \pi^+ n$  process as a function of  $-t$  for four different center-of-mass energies: 2.67, 2.95, 3.36, 3.87 GeV. The black solid curve is the Regge prediction discussed in the text and the red stars are from Zhu *et al.* [7]. All other data are shown as solid squares [39], solid circles [40], solid triangles [41], and open circles [24, 42]. The black dotted line is based on the CCR.

can be easily identified at all energies. The bottom left panel shows the broad center-of-mass angular distribution for all single pion events, while the bottom right panel shows the angular coverage for pions from the process  $\gamma p \rightarrow \pi^+ n$  (selected by putting a cut around the neutron mass in the missing mass spectrum).

Figure 12 shows the number of  $\gamma p \rightarrow \pi^+ n$  events as a function of photon energy (for 150 MeV bins) for various  $10^\circ$  angular bins around the central C.M. angle of  $50^\circ$ ,  $70^\circ$ ,  $90^\circ$  and  $120^\circ$  respectively. These spectra are used to estimate the number of events that will be collected during the proposed experiment.

### Monte Carlo Simulation

We performed Monte Carlo simulations of the proposed experiment using the CLAS simulation package GSIM [45] and the event generator GENBOS [46]. All possible positive particle production channels for a hydrogen target were included in the event generator.

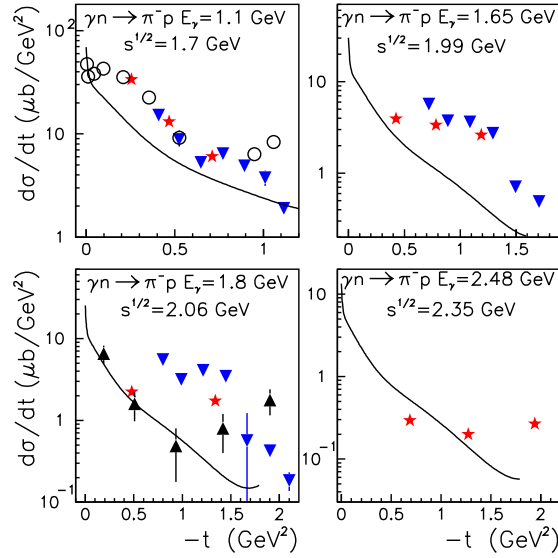


FIG. 9: The differential cross-section  $\frac{d\sigma}{dt}$  for the  $\gamma n \rightarrow \pi^- p$  process as a function of  $-t$  for four different center-of-mass energies: 1.7, 1.99, 2.06, 2.35 GeV. The black solid curve is the Regge prediction discussed in the text and the red stars are from Zhu *et al.* [7]. All other data are shown as open circles [43], solid inverse triangles [26], and solid triangles [44]

The simulations were performed at  $B = B_{max}$  ( $I = 3375$  A) and at  $B = 0.5 \times B_{max}$  ( $I = 1920$  A) and compared to help decide the optimal running conditions. The results of the simulation are shown in Figures 13 - 15. Fig. 13 shows the missing mass spectrum for all positive pion events detected, it also shows (in red) the cut around the neutron mass that was used to select the  $\gamma p \rightarrow \pi^+ n$  events. The right panel is for  $B = 0.5 \times B_{max}$  while the left panel is for  $B = B_{max}$ . Fig. 14 shows the lab angle and momentum distributions of the detected pions. The panels on the left are for all detected  $\pi^+$  events while the ones on the right are for events which have a missing mass within a narrow cut around the neutron mass. The blue histograms are for  $B = 0.5 \times B_{max}$  while the red ones are for  $B = B_{max}$ . These results clearly show that at  $B = B_{max}$  the acceptance for the background is reduced (see Fig. 13) without effecting the acceptance for the  $\gamma p \rightarrow \pi^+ n$  channel (see Fig. 14). Thus we have chosen to run this experiment at  $B = B_{max}$ . In Figure 15 we have show the simulated signal to background ratio. This ratio for  $E_\gamma < 3.85$  GeV was normalized to the data from

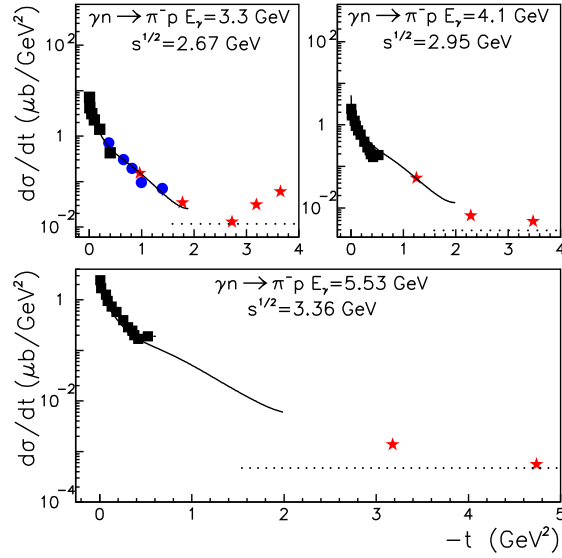


FIG. 10: The differential cross-section  $\frac{d\sigma}{dt}$  for the  $\gamma n \rightarrow \pi^- p$  process as a function of  $-t$  for four different center-of-mass energies: 2.67, 2.95, 3.36 GeV. The black solid curve is the Regge prediction discussed in the text and the red stars are from Zhu *et al.* [7]. The data from [39, 40] are shown as solid circles and solid squares, respectively. The black dotted line is based on the CCR.

g11 running period taken with single charged particle trigger (red histogram in Fig. 15). The simulations suggest that the signal to background is almost flat between 4 and 5.4 GeV and since one is able to separate the signal from the background at 4 GeV (as shown in Fig. 11) this experiment is feasible.

## THE EXPERIMENT

### Overview

We propose to use the Hall B bremsstrahlung tagged photon beam and the CLAS detector with a 40 cm long cryogenic liquid hydrogen target placed at the center of CLAS. The bremsstrahlung photon beam will be produced with a gold radiator having a thickness of  $10^{-4}$  radiation lengths. We request an electron beam energy  $E_0 = 5.7$  GeV and a current of 25 nA. The entire CLAS tagger will be read out during data taking, covering from 20% to 95% of the electron beam energy, i.e. (1.14 – 5.4) GeV. The full tagger together Start

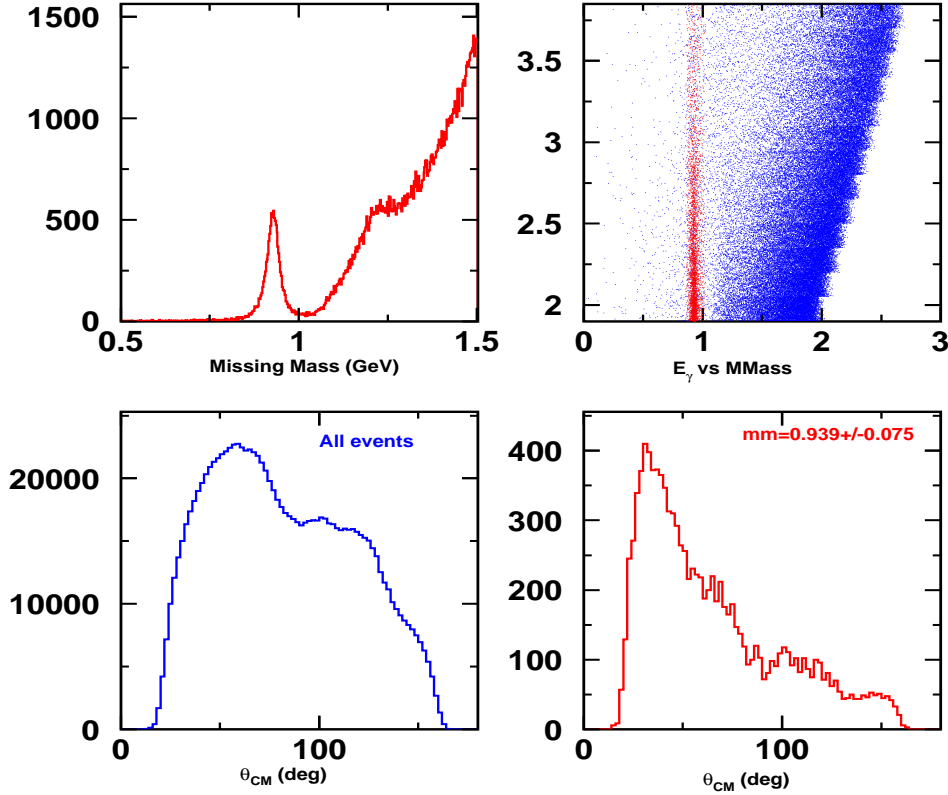


FIG. 11: Sample spectra from g11 run 44013 which had a single charge particle trigger. Upper left panel is the missing mass spectrum for  $\pi^+$  events. Upper right panel is the missing mass versus photon energy. Lower left panel is angular distribution for all pion events and lower right panel is the angular distribution for  $\gamma p \rightarrow \pi^+ n$  events.

Counter (ST) and CLAS will trigger the data acquisition, covering the entire range of photon energies available. Since we are interested in final states with only one charged particles we will require the detection of at least one positively charged particles in CLAS. Finally an in-bending torus field of  $B = B_{max}$  ( $I = 3375$  A) will be requested.

### Tagger rate

Under the above experimental conditions the rate of the entire tagger will be  $\sim 24.3 \times 10^6 \gamma/s$ . This corresponds to a rate of  $\sim 63$  kHz on each E-counter and  $\sim 400$  kHz on each T-counter. The rate of multiple hits in the tagger can be estimated as

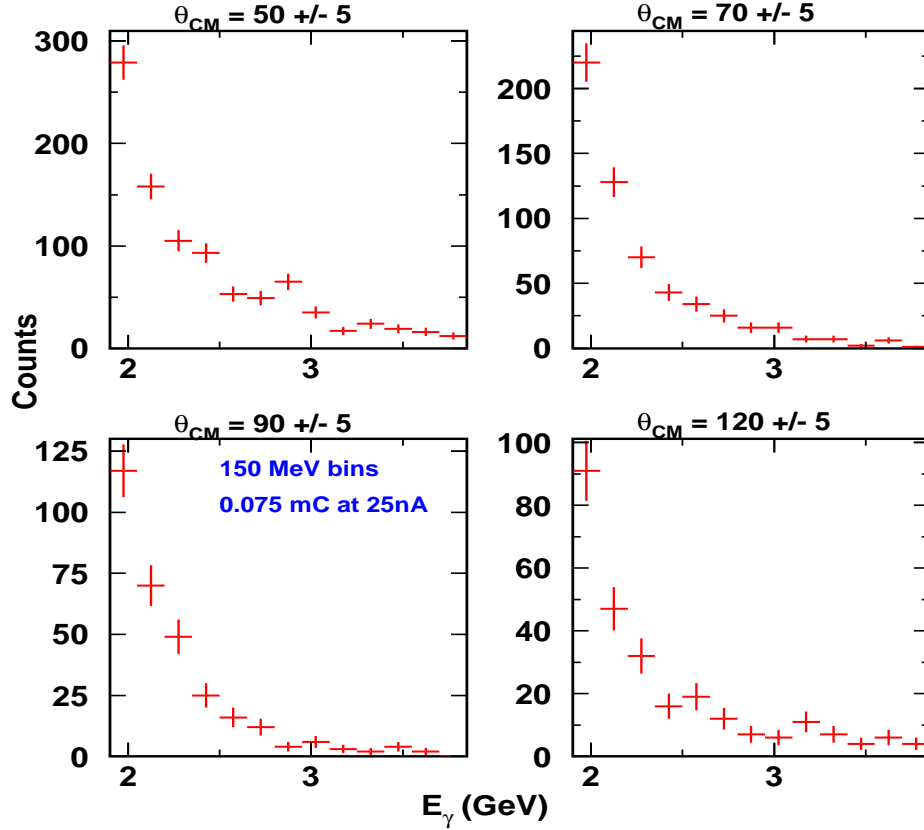


FIG. 12: Yield as function of photon energy for the  $\gamma p \rightarrow \pi^+ n$  process at  $\theta_{cm} = 50^\circ, 70^\circ, 90^\circ, 120^\circ$  obtained from a single g11 run (with single charge particle trigger).

$$R_{tagger}^{multiplehits} = 2 \times \Delta\tau \times \phi_\gamma \times \phi_\gamma \simeq 2400 \text{ kHz} \quad (2)$$

where the coincidence time of  $\Delta\tau = 2$  ns reflects the time resolution achievable in the off-line analysis. This rate corresponds to  $\sim 15\%$  of the MOR (master OR) rate and it is an acceptable value. Since we do not detect the recoil neutron we cannot recover these events, we propose to drop these events and correct for them.

### CLAS, Start Counter and MOR: Trigger rates and accidentals

The relevant hadronic rate comes from photons (mainly untagged) above the pion threshold ( $E_\gamma > 140$  MeV) which corresponds to  $58 \times 10^6 \gamma/s$ . This means that, assuming a

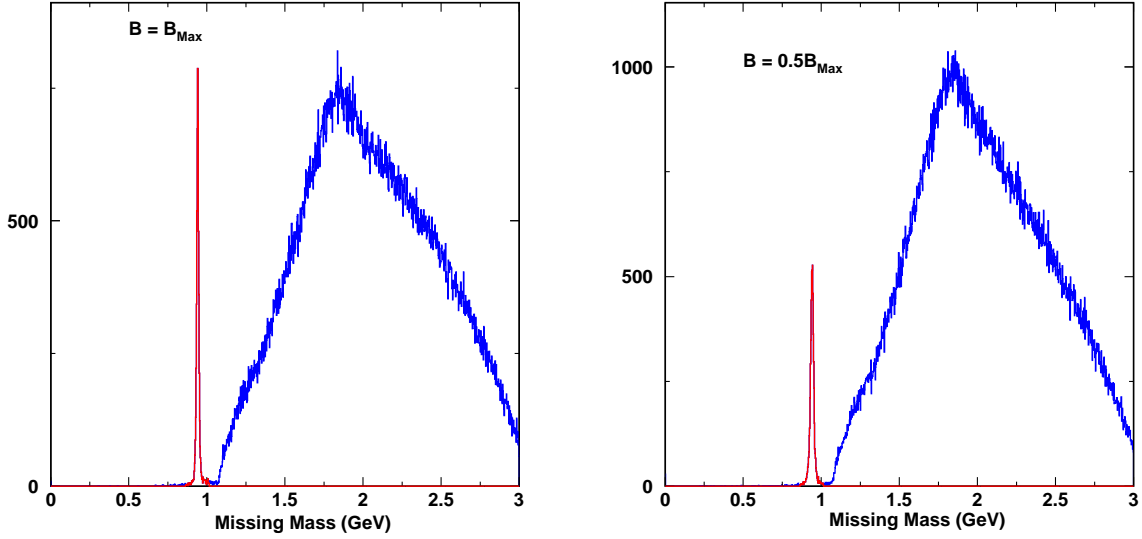


FIG. 13: The missing mass spectra from a simulation of positive pion production from hydrogen. Right panel is for  $B = 0.5 \times B_{max}$  while the left panel is for  $B = B_{max}$

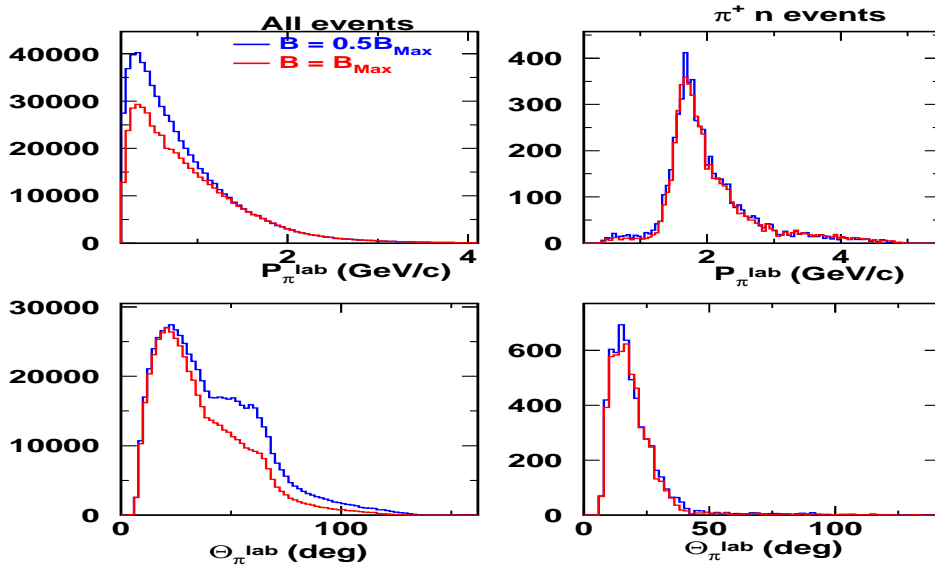


FIG. 14: The simulated lab momentum and angular distributions of events. The panels on the left are for all positive charged particle ( $\pi$ , K, P) events produced on hydrogen, while the panels on the right are for only the  $\pi^+$  events which have a missing mass around the neutron mass. The blue histograms are for  $B = 0.5 \times B_{max}$  while the red are for  $B = B_{max}$ .

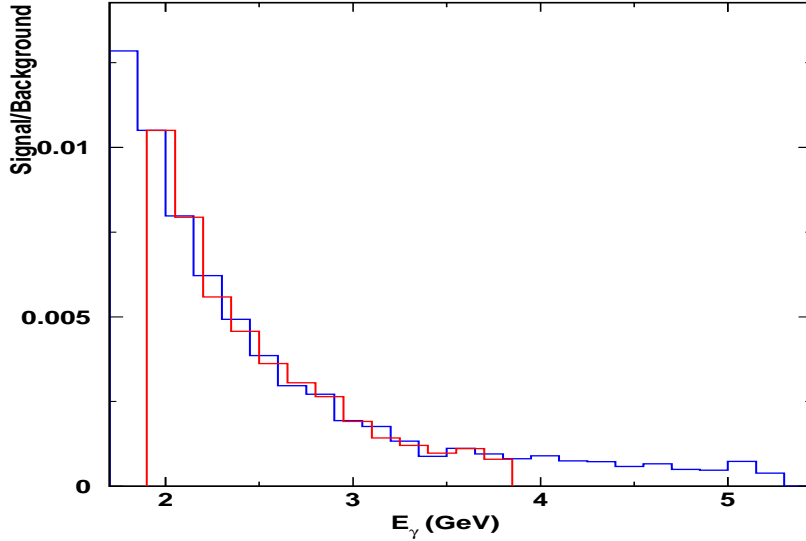


FIG. 15: The simulated signal to background ratio (blue), that was normalized to g11 data (run 44013, with single charged particle trigger) for  $E_\gamma < 3.85$  GeV shown in red.

photo-absorption cross section of  $\sigma_{hadron} = 150 \mu barn$  [47]

$$R_{hadron} = \phi_\gamma(E_\gamma > \pi) \cdot T_{length} \cdot \rho \cdot N \cdot \sigma_{hadron} \simeq 15 kHz \quad (3)$$

where  $T_{length} = 40$  cm is the target length,  $N = 6.02 \times 10^{23}$  is the Avogadro's number and  $\rho = 0.0708 gr/cm^3$  is the liquid hydrogen density. Approximately 44% of these events comes from tagged photons and the remaining 56% from untagged photons [48]. All these events will produce a hit in the Start Counter, which is almost 100% of acceptance, while CLAS will see only  $\sim 60\%$  of them (we have evaluated this number considering  $\sim 90\%$  for the single particle detection efficiency and  $\sim 70\%$  for the CLAS acceptance).

In addition to the hadronic events, the Start Counter will also be affected by the electromagnetic background produced by the photon beam. Based on the work of [49] and from g11 experiment, this electromagnetic background could be estimate of the order of  $\sim 7$  MHz. To estimate the trigger rate and the accidentals we will proceed in two steps: first we will consider the MOR  $\times$  ST coincidence rate and then the (MOR  $\times$  ST)  $\times$  CLAS one.

- MOR  $\times$  ST

The MOR will be used in coincidence with the Start Counter within a 10 ns coincidence window. The MOR  $\times$  ST coincidence rate will be affected by two type of accidentals:

- 1) Hadronic events in the Start Counter induced by photons which are below the minimum triggered energy of 1.14 GeV;
- 2) hits in the Start Counter induced by electromagnetic background.

Assuming a coincidence window of  $\Delta\tau = 10$  ns, we have:

$$R_{MORXST}^{acc1} = 2 \cdot \Delta\tau \cdot \phi_{tagged} \cdot (R_{ST}^{hadr} - R_{ST}^{hadr}(tagged)) \simeq 4.0 \text{ kHz} \quad (4)$$

where  $R_{ST}^{hadr} = 15$  kHz

$$R_{MORXST}^{acc2} = 2 \cdot \Delta\tau \cdot \phi_{tagged} \cdot R_{ST}^{BG} \simeq 580 \text{ kHz} \quad (5)$$

where for  $R_{ST}^{BG}$  a value of 1.2 MHz has been chosen, because, the segmentation of the new Start Counter allows for a configuration in which groups of 6 scintillators could be put in coincidence with each CLAS sector. Thus the total 7 MHz has been divided by 6.

- MOR  $\times$  ST  $\times$  CLAS

After requiring the coincidence with CLAS, the first accidental rate will be reduced by the CLAS acceptance and efficiency while, on the contrary, the second rate will be reduced to a greater extent, since it is uncorrelated with CLAS.

Assuming a coincidence window  $\Delta\tau = 100$  ns, the final accidental rates are estimated to be:

$$R_{(MORXST)XCLAS}^{acc1} = R_{MORXST}^{acc1} \cdot Eff_{CLAS} \simeq 2.4 \text{ kHz} \quad (6)$$

$$R_{(MORXST)XCLAS}^{acc2} = 2 \cdot \Delta\tau \cdot R_{MORXST}^{acc2} \cdot (R_{ST}^{hadr} - R_{ST}^{hadr}(tagged)) \cdot Eff_{CLAS} \simeq 590 \text{ Hz} \quad (7)$$

The total DAQ rate is then:

$$R_{trigger} = R_{hadr}^{true} \cdot Eff_{CLAS} + R_{(MORXST)XCLAS}^{acc1} + R_{(MORXST)XCLAS}^{acc2} \simeq 6.9 \text{ kHz} \quad (8)$$

which is within the DAQ limits.

Moreover, the recent improvements in the DAQ makes it possible to run with trigger rates of 8 -9 KHz with low deadtime [50]. This has been demonstrated during the g13 running where a 10-12% deadtime was observed at a trigger rate of 8 KHz [51]. In the off-line data analysis the "true" events will be extracted from the total recorded events using a tighter

time coincidence between Start Counter and MOR. This software coincidence window is set to 1 ns and will reduce the accidental rate to  $\simeq 200$  Hz and to  $\simeq 48$  Hz respectively. The final contamination to the true rate due to accidentals is therefore estimated to be less than 10%.

### Counting Rates and Beam Time Estimate

Based on the sample spectra obtained from run 44013 of the g11 running period, we can estimate the number of events we can expect to get in 100 hours of running with a 25 nA beam on a 40 cm liquid hydrogen target. We have estimated the expected yield for  $10^\circ$  bins around the C.M. angles of  $50^\circ$ ,  $70^\circ$ ,  $90^\circ$  and  $120^\circ$ . The yield is determined for each photon energy bin (150 MeV wide) based on the rates shown in Figure 12. For photon energy beyond 3.8 GeV the yield is estimated by assuming  $s^{-7}$  scaling. These rates were found to be consistent with the rates measured in the previous experiment (E94-104) at  $70^\circ$  and  $90^\circ$ . For the  $50^\circ$  case however, the scaling assumption under-estimates the yields.

We have also carried out a preliminary study of the feasibility of running the proposed experiment concurrently with the g12 experiments. There are in principle two possibilities: (1) running with an additional single charged particle trigger with a prescaling factor; (2) adding a second trigger with one charged particle in CLAS and one neutral particle in the opposite sector from the Electromagnetic Calorimeter (EC + LAC). For the proposed experiment, precise knowledge of the photon flux is crucial for the extraction of the differential cross-section. Therefore, we want to avoid multiple triggers because of the potential ambiguities in determination of the photon flux. There are also potential issues both in the extraction of cross-section from prescaled data, and in the determination of the neutral particle detection and trigger efficiencies. Moreover, a trigger with a neutral particle in the EC dramatically reduces the angular coverage at forward angles which is undesirable for this experiment. Therefore, our conclusion is to request for 4 days of dedicated beam time for the proposed experiment with a current of 25 nA and a beam energy of 5.7 GeV with a dedicated single charged particle trigger in CLAS.

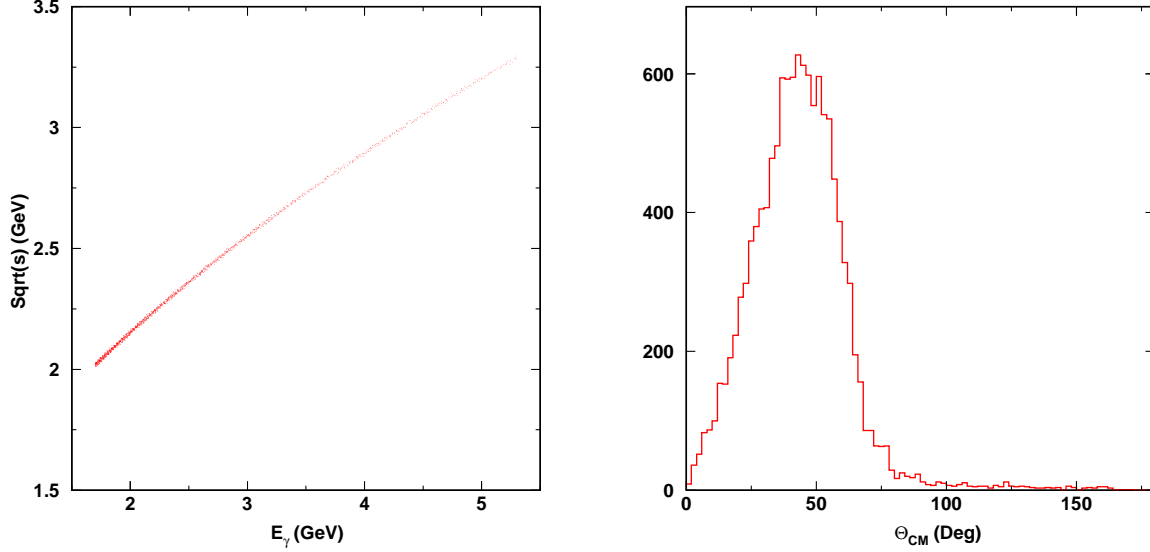


FIG. 16: The center of mass energy  $\sqrt{s}$  vs the incident photon energy for the simulated  $\gamma p \rightarrow \pi^+ n$  events (left). The simulated coverage of the pion center of mass angle (right).

### Projected Results

The expected coverage in the center of mass energy  $\sqrt{s}$  and angle  $\theta_{CM}$  are shown in Figure 16. The projected results for a fraction of the entire angular coverage  $\theta_{cm}$  centered from  $50^\circ$  to  $115^\circ$ , are shown in Figure 17. Only the statistical uncertainties are shown in these projections.

### SUMMARY

We have proposed a measurement of the  $\gamma p \rightarrow \pi^+ n$  reaction using the CLAS detector. With an energy beam of  $E_0 = 5.7$  GeV we plan to map out the region of  $\sqrt{s} = 1.77 - 3.32$  GeV in fine steps of approximately 0.15 GeV and also perform an angular scan in steps of  $10^\circ$ . These measurements would i) help understand the dramatic enhancement and rapid drop in the scaled cross-section observed in the E94-104 data and ii) provide information on the onset of scaling behavior over a wide angular range, and iii) test the possible oscillatory behavior of the scaled free space differential cross-sections about the quark counting prediction. We will use the standard Hall B equipment along with the radiator and tagger. The Hall B cryogenic 40 cm liquid hydrogen target will be used. A total of 100 hours (4 days) of beam

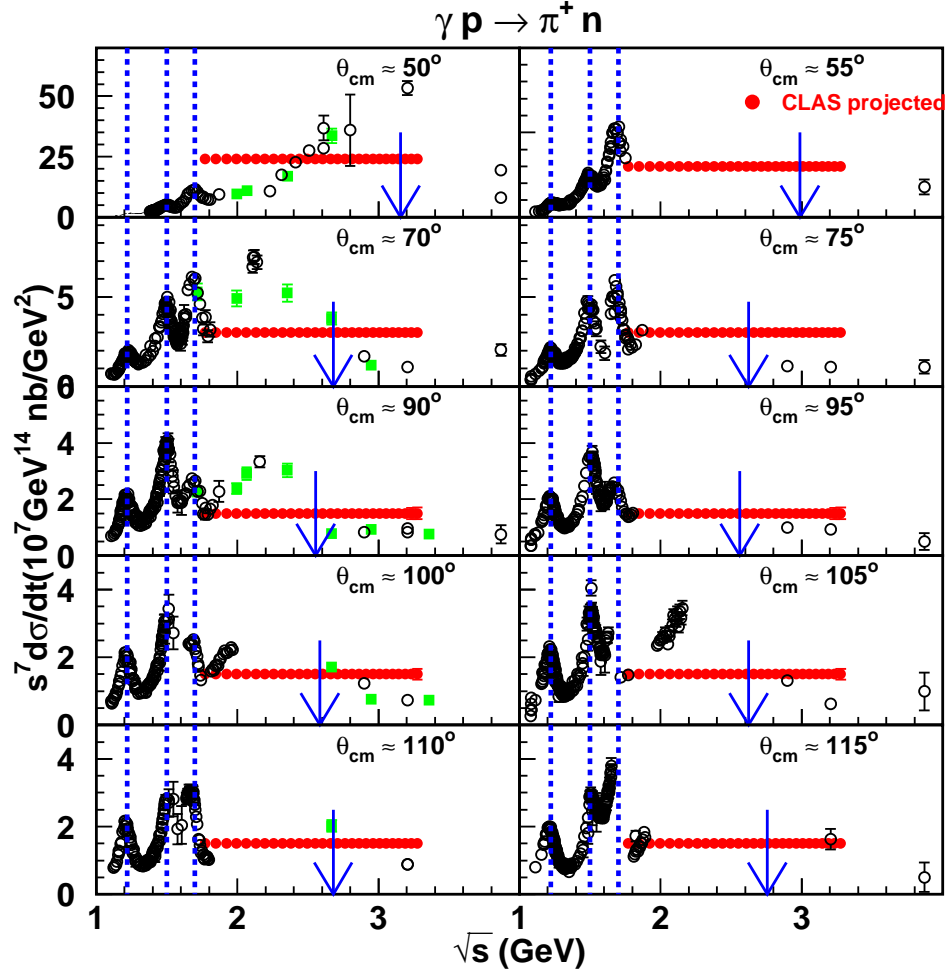


FIG. 17: Projected results for the  $\gamma p \rightarrow \pi^+ n$  process as a function of  $\sqrt{s}$  for different pion center-of-mass angle.

time will be required for this experiment.

#### ACKNOWLEDGMENTS

We thank P. Eugenio, T.S.-H. Lee, B. Mecking, A. Sibirtsev, P. Nadel-Turonski, E. Pasyuk, P. Stoler, and D. Weygand for helpful discussions.

- 
- [1] S.J. Brodsky and G.R. Farrar, Phys. Rev. Lett. **31**, 1153 (1973); Phys. Rev. D **11**, 1309 (1975); V. Matveev *et al.*, Nuovo Cimento Lett. **7**, 719 (1973);
- [2] R. L. Anderson *et al.*, Phys. Rev. D **14**, 679 (1976); C. White *et al.*, Phys. Rev. **D49**, 58 (1994).
- [3] J. Napolitano *et al.*, Phys. Rev. Lett. **61**, 2530 (1988); S.J. Freedman *et al.*, Phys. Rev. C **48**, 1864 (1993); J.E. Belz *et al.*, Phys. Rev. Lett. **74**, 646 (1995).
- [4] C. Bochna *et al.*, Phys. Rev. Lett. **81**, 4576 (1998).
- [5] E.C. Schulte, *et al.*, Phys. Rev. Lett. **87**, 102302 (2001);
- [6] P. Rossi *et al.*, Phys. Rev. Letts. **94**, 012301 (2005); M. Mirazita *et al.*, Phys. Rev. C **70**, 014005 (2004).
- [7] L. Y. Zhu *et al.*, Phys. Rev. Lett. **91**, 022003 (2003); L. Y. Zhu *et al.* Phys Rev. C, **71**, 044603 (2005).
- [8] K. Wijesooriya, *et al.*, Phys. Rev. Lett. **86**, 2975 (2001); X. Jiang *et al.*, Phys. Rev. Lett. **98**, 182302 (2007).
- [9] W. Chen *et al.*, to be published.
- [10] M. Dugger *et al.*, Phys. Rev. C **76**, 025211 (2007).
- [11] H. Genzel, P. Joos, and W. Pfeil, Photoproduction of Elementary Particles (Springer-Verlag, Berlin, 1973), Group I Volume 8 of Numerical Data and Functional Relationships in Science and Technology, edited by K.-H. Hellwege.
- [12] P. V. Landshoff, Phys. Rev. D **10**, 1024 (1974).
- [13] J. Polchinski and M.J. Strassler, Phys. Rev. Lett. **88**, 031601 (2002); R.C. Brower and C.I. Tan, Nucl. Phys. B **662**, 393 (2003); O. Andreev, Phys. Rev. D **67**, 046001 (2003).
- [14] A.W. Hendry, Phys. Rev. D **10**, 2300 (1974).
- [15] D.G. Crabb *et al.*, Phys. Rev. Lett. **41**, 1257 (1978).
- [16] G.R. Court *et al.*, Phys. Rev. Lett. **57**, 507 (1986), T.S. Bhatia *et al.*, Phys. Rev. Lett. **49**, 1135 (1982), E.A. Crosbie *et al.*, Phys. Rev. D **23**, 600 (1981).
- [17] S.J. Brodsky, C.E. Carlson, and H. Lipkin, Phys. Rev. D **20**, 2278 (1979).
- [18] J.P. Ralston and B. Pire, Phys. Rev. Lett. **61**, 1823 (1988), J.P. Ralston and B. Pire, Phys. Rev. Lett. **65**, 2343 (1990).

- [19] C.E. Carlson, M. Chachkhunashvili, and F. Myhrer, Phys. Rev. D **46**, 2891 (1992).
- [20] S. J. Brodsky, and G. F. de Teramond, Phys. Rev. Lett. **60**, 1924 (1988).
- [21] Q. Zhao and F. E. Close, Phys. Rev. Lett. **91**, 022004 (2003).
- [22] X. Ji, J.-P. Ma and F. Yuan, Phys. Rev. Lett. **90**, 241601 (2003).
- [23] S. J. Brodsky and G. F. de Teramond, Phys. Lett. **B582**, 211 (2004); S. J. Brodsky *et al.*, Phys. Rev. D **69**, 076001 (2004).
- [24] R.L. Anderson *et al.*, Phys. Rev. **D14**, 679 (1976).
- [25] O. Bartholomy *et al.*, Phys. Rev. Lett. **94**,012003 (2005).
- [26] H.-J. Besch *et al.*, Z. Phys. C **16**, 1 (1982).
- [27] I. I. Strakovsky (private communication); R. A. Arndt *et al.*, Phys. Rev. **C66**, 055213 (2002); nucl-th/0205067; <http://gwdac.phys.gwu.edu/>.
- [28] I. I. Strakovsky (private communication); S. S. Kamalov, *et al.*, Phys. Rev. C **64**, 032201 (2001)(A dynamical model); D. Drechsel, *et al.*, Nucl. Phys. A **645**, 145 (1999)(a unitary isobar model); MAID2001 refers to the Nov. 2001 version of the MAID solution from S. S. Kamalov.
- [29] S. Capstick, Phys. Rev. D **46**, 2864 (1992); S. Capstick and W. Roberts, Phys. Rev. D **49**, 4570 (1994).
- [30] The BES Collaboration, M. Ablikim *et al.*, Phys. Rev. Lett. **97**, 062001 (2006).
- [31] V. Credé, *et al.*, Phys. Rev. Lett. **94**, 012004 (2005).
- [32] S.J. Brodsky, I.A. Schmidt, G.F. de Teramond, Phys. Rev. Lett. **64**, 1011 (1990).
- [33] H. Gao, T.S.-H. Lee, and V. Marinov, Phys. Rev. C **63**, 022201(R) (2001).
- [34] F. Huang, Z.Y. Zhang, and Y.W. Yu, Phys. Rev. C **73**, 025207 (2006).
- [35] A. Sibirtsev, J. Haidenbauer, S. Krewald, T.-S.H. Lee, U.-G. Meissner, and A.G. Thomas, Nucl-th/07060183.
- [36] J.P. Dowd, D.O. Caldwell, K. Heinloth and T.R. Sherwood, Phys. Rev. Lett. **18**, 414 (1967).
- [37] G. Buschhorn *et al.*, Phys. rev. Lett. **17**, 1027 (1966); G. Buschhorn *et al.*, Phys. rev. Lett. **18**, 571 (1967).
- [38] S.D. Ecklund and R.L. Walker, Phys. Rev. **159**, 1195 (1967).
- [39] P. Heide *et al.*, Phys. Rev. Lett. **21**, 248 (1968).
- [40] Z. Bar-Yam *et al.*, Phys. Rev. Lett. **19**, 40 (1967).
- [41] A.M. Boyarski *et al.*, Phys. Rev. Lett. **20**, 300 (1968).
- [42] R.L. Anderson *et al.*, Phys. Rev. Lett. **23**, 721 (1969).

- [43] P.E. Scheffler and P.L. Walden, Nucl. Phys. B **75**, 125 (1974).
- [44] P. Benz *et al.*, Nucl. Phys. B **65**, 158 (1973).
- [45] M. Guidal *et al.*, CLAS-note 93-013
- [46] A. S. Iljinov *et al.*, Nucl. Phys. A **616**, 575 (1997)
- [47] W.-M. Yao *et al.*, Journal of Phys., G **33**, 1 (2006).
- [48] D. I. Sober *et al.*, Nucl. Inst. and Meth. A**44**, 263 (2000).
- [49] M. Guidal *et al.*, CLAS-note 95-009.
- [50] S. Stepanyan, private communication.
- [51] E. Pasyuk, private communication.